Engineering of an alternative electron transfer path in photosystem II

Shirley Larom[a,1], Faris Salama[b,1], Gadi Schuster[a], and Noam Adir[b,2]

[a]Faculty of Biology and [b]Schulich Faculty of Chemistry, Technion-Israel Institute of Technology, Haifa 32000, Israel

Edited* by Harry B. Gray, California Institute of Technology, Pasadena, CA, and approved April 15, 2010 (received for review January 6, 2010)

The initial steps of oxygenic photosynthetic electron transfer occur within photosystem II, an intricate pigment/protein transmembrane complex. Light-driven electron transfer occurs within a multistep pathway that is efficiently insulated from competing electron transfer pathways. The heart of the electron transfer system, composed of six linearly coupled redox active cofactors that enable electron transfer from water to the secondary quinone acceptor Q_B, is mainly embedded within two proteins called D1 and D2. We have identified a site *in silico*, poised in the vicinity of the Q_A intermediate quinone acceptor, which could serve as a potential binding site for redox active proteins. Here we show that modification of Lysine 238 of the D1 protein to glutamic acid (Glu) in the cyanobacterium *Synechocystis* sp. PCC 6803, results in a strain that grows photoautotrophically. The Glu thylakoid membranes are able to perform light-dependent reduction of exogenous cytochrome c with water as the electron donor. Cytochrome c photoreduction by the Glu mutant was also shown to significantly protect the D1 protein from photodamage when isolated thylakoid membranes were illuminated. We have therefore engineered a novel electron transfer pathway from water to a soluble protein electron carrier without harming the normal function of photosystem II.

cyanobacteria | energy conversion | proinhibition | photosynthesis | protein engineering

Photosynthesis is the major source of useful chemical energy in the biosphere. All photosynthetic processes require efficient electron transfer (ET) pathways that are utilized for proton gradient formation (to be used for the production of ATP) and/or accumulation of reducing equivalents (1, 2). Light energy, absorbed by light-harvesting antenna complexes, is transferred to photochemical reaction centers (RC), initiating charge separation in specific chlorophyll molecules bound to the RC proteins. Following charge separation, electrons are transferred sequentially to a series of acceptor molecules, each with a redox potential determined by its immediate environment (3, 4). The source of electron replenishment differs according to the reaction center type. For instance in purple non-sulfur bacteria, electrons are cycled back to the oxidized reaction center by a soluble cytochrome c (cyt c) type protein (5, 6). Oxygenic photosynthetic organisms (cyanobacteria, red and green algae and plants) contain two photosystems: photosystem I (PSI) and photosystem II (PSII) that work linearly (1, 7), and the source of electrons is water. One common facet of all ET pathways is the requirement for insulation of the redox active cofactors from potentially reducing/oxidizing molecules within the RC or in the surrounding media. Insulation provides the system with maximal ET rates and efficiencies and also prevents damage to the RC.

PSII has a redox potential of up to 1.2 V (8, 9), required to abstract electrons from water (Fig. 1*A*). The photoexcited P_{680} reaction center chlorophyll *a* primary donor transfers electrons via pheophytin *a* and a plastoquinione (PQ) intermediate (Q_A) molecule to finally doubly reduce a second, transiently bound PQ molecule (Q_B). Q_B^{2-} is doubly protonated and released from the RC as PQH_2 into the membrane. The lifetime of Q_A^- is about 100 μsec in the presence of oxidized Q_B, while in the presence of Q_B site inhibitors, such as 3-(3,4-dichlorophenyl)-1,1-dimethylurea (DCMU), the lifetime of Q_A^- can be on the order of seconds (10). The redox potential of Q_A/Q_A^- is altered by the presence of the Q_B site inhibitors (11), showing that small structural changes in the PSII RC can change the electrochemical properties of the cofactors. The long-lived presence of Q_A^- may increase the possibility of formation of doubly reduced Q_A molecule (Q_A^{2-}), which may be one of the reasons for the phenomenon known as photoinhibition (PI) (12). Under normal conditions of illumination, the D1 protein of the RC core is irreversibly damaged over time requiring its replacement in a fashion that preserves the integrity of the PSII complex (12). PI occurs if the rate of D1 damage exceeds the rate of replacement, leading to loss of photosynthetic viability. Because the lifetime of Q_A^- can be extensive, it appears that the Q_A binding site is efficiently insulated, and electrons are usually not lost to alternative oxidizing pathways, in vivo.

Synthetic and semisynthetic energy conversion systems, based on photosynthetic processes, have recently been proposed (8, 13–15). These include attempts to use dyes bound to solid-state materials, coupled molecules that form novel ET pathways and the growth of photosynthetic organisms [plants, green algae, cyanobacteria, (16–18)], which are then converted to biofuels (19–21). An additional approach could be the use of a native and viable photosynthetic system adapted to serve as a direct source of either sustained electrical current or storable chemical energy. Here, we show that by changing one amino acid in the D1 PSII protein, located at the vicinity of the Q_A, a novel ET pathway is created in which electrons are withdrawn from Q_A to an artificially added soluble cyt c. Therefore, a native photosynthetic organism can be modified in a fashion that does not prevent photoautotrophic growth but contains a novel, and perhaps useful, conduit for ET.

Results

***In Silico* Analysis of the Cytoplasmic-Facing Surface of PSII Identifies a Potential Protein Binding Site.** PSII performs linear electron transfer from H_2O to the secondary acceptor, Q_B (22). The redox active components from Y_Z to Q_B are embedded within the D1 and D2 proteins, while the oxygen evolving center (OEC) is bound to the luminal face of PSII (Fig. 1*A*). PSII has physical and functional similarities to the bacterial reaction center of *Rb. sphaeroides* (bRC) (5). However unlike PSII, the bRC serves as a component of a cyclic electron transfer system that contains a conduit for electron transfer donation from a soluble cytochrome c_2 (cyt c2) to the oxidized donor, P_{860}^+ (6). The binding of cyt c2 to the bRC has been studied in the past, and the binding site has been determined by X-ray crystallography (23, 24). The cyt c2

Author contributions: S.L., F.S., G.S., and N.A. designed research; S.L. and F.S. performed research; S.L., F.S., G.S., and N.A. analyzed data; and G.S. and N.A. wrote the paper.

The authors declare a conflict of interest. A preliminary patent has been filed via the Technion Research and Development Foundation Ltd.

*This Direct Submission article had a prearranged editor.

[1]S.L. and F.S. contributed equally to this work.

[2]To whom correspondence should be addressed. E-mail: nadir@tx.technion.ac.il.

This article contains supporting information online at www.pnas.org/lookup/suppl/doi:10.1073/pnas.1000187107/-/DCSupplemental.

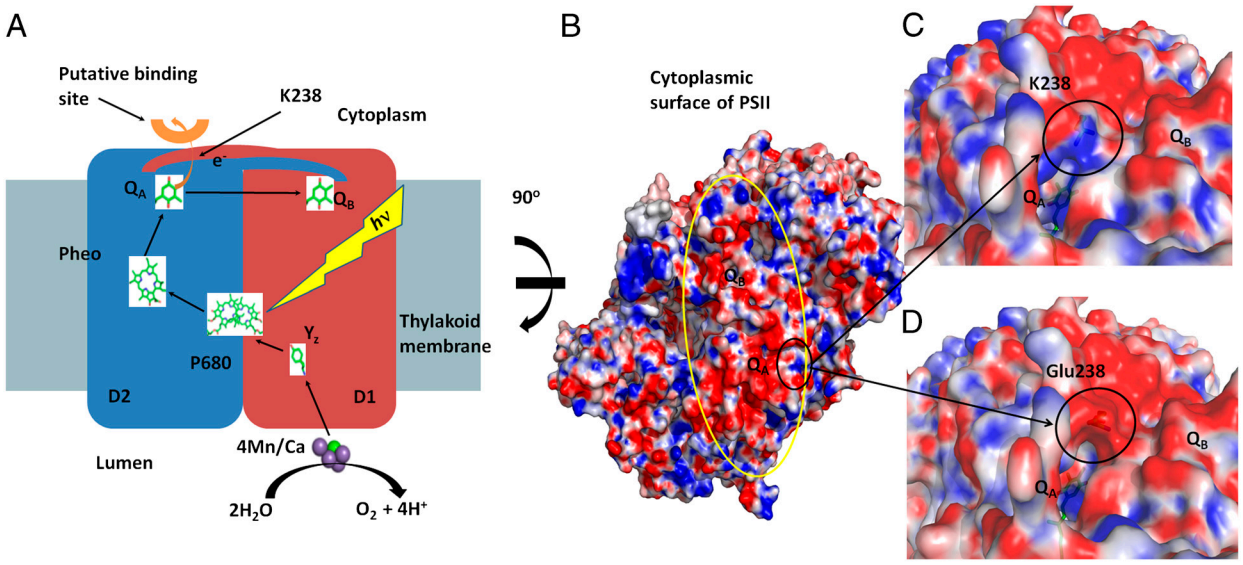

Fig. 1. *In silico* analysis of the cytoplasmic-facing surface of PSII reveals the amino acid to be targeted for engineering the unique electron transfer conduit. (*A*) Schematic model of monomeric PSII reaction center. Only electron transfer chain cofactors are depicted. Black arrows within the complex indicate the direction of electron flow from the H_2O to Q_B. Orange arrow and curved surface indicate potential position of engineered electron transfer pathway. The D1 and D2 proteins crossover each other on the cytoplasmic surface, and the position of D1-K238 is indicated. (*B*) Electrostatic potential mapped onto the cytoplasmic face of wild type PSII using the 3BZ1 crystal structure. Red and blue indicate negative and positive potentials (±15 kT/e), respectively. The PSII reaction center is identified by the yellow oval; Q_A and Q_B indicate the sites of these two quinone acceptors (~ 10 Å below the surface). The K238 site is identified by the black oval. (*C*) Close-up of the K238 potential (black oval) positioned above the Q_A site (sticks). (*D*) Calculated electrostatic potential mapped onto the cytoplasmic surface of the Glu virtual mutant. Notice the negative potential that now appears at position 238 (black oval). See *Materials and Methods* for details on potential calculation and visualization.

binding site has a significant negative electrostatic potential which is complementary to the positive electrostatic potential of the cyt c2 surface adjacent to the heme cofactor. The binding affinity of cyt c2 to the bRC has been estimated to be on the order of 0.1–1 μM (25), and there is an excess of cyt c2 in *Rb. sphaeroides* cells, assuring a high turnover rate.

PSII has two surfaces on either side of the thylakoid membrane. The surface occupied by the OEC is sequestered within the thylakoid lumen space (Fig. 1*A* and Fig. S1) (26, 27). The PSII surface that faces the cytoplasm is rather flat (Fig. S1) and could potentially interact with redox active soluble proteins. In cyanobacteria, this surface is at least partially occupied by the phycobilisome light-harvesting antenna, while in green algae and plants it participates in the formation of the grana stacks. Thus, spurious binding of redox proteins may be limited, in vivo. Isolated thylakoid membranes however, could present the cytoplasmic surface to ET proteins, essentially "short-circuiting" the natural flow of electrons. We examined the cytoplamic surface of cyanobacterial PSII using the recently available crystal structures (26–28). Fig. 1*B* shows the calculated electrostatic potential of the PSII surface facing the cytoplasm. From this vantage point, it can be seen that the surface above the Q_A acceptor is more negative than the surface above Q_B. A small patch of positive potential within the larger negative potential located above Q_A (Fig. 1*C*) is due to the presence of D1-lysine 238 (K238). Interestingly, this position is either a lysine or an arginine in all oxygenic photosynthetic organisms (Fig. S2). Because K238 is located on the surface closest to Q_A, engineering a binding site here could bring an electron acceptor to within 15–20 Å of Q_A. At this distance, the kinetics of ET from Q_A^- would most likely be within the μsec range (29). We virtually mutagenized K238 to either neutral or acidic residues, with different molecular volumes. Fig. 1*D* shows that the positive patch in the calculated electrostatic potential of the virtual mutant K238E (Glu) was abolished. Neutral mutations to alanine or leucine (Ala or Leu, respectively) had a less negative surface potential than the Glu mutant, as expected.

Engineering and Characterization of the Electron Conduit. On the basis of the *in silico* analysis we decided to perform site-specific mutagenesis that will replace the conserved K238 with neutral or negative amino acids. The cyanobacterium *Synechocystis* sp. PCC 6803 (*Syn*) is amenable to site-specific mutagenesis and photoautotrophic/heterotrophic selection procedures. The *Syn* genome contains a gene family of three *psbA* genes encoding the D1 protein. The *psbA2* and *psbA3* genes encode for an identical D1 protein (D1m), with *psbA2* providing about 90% of the transcript under normal growth conditions (30). If either *psbA2* or *psbA3* is inactivated, the remaining gene is sufficient to enable photoautotrophic growth and express the full quantity of the D1 protein (30). *psbA1* potentially encodes a D1 protein that is different in three amino acids (D1′) and has been considered as a pseudogene (30). In the TD34 *Syn* strain, each of the three *psbA* genes has been replaced by antibiotic resistance cassettes (31). This enables the replacement of a single cassette with a wt or mutated copy of *psbA*, using heterologous recombination (Fig. S3*C*). The resulting mutants can either be grown on glucose or in a photoautotrophic manner. Three different mutations were introduced into the *psbA3* gene K238 site, changing the lysine to an alanine, glutamic acid, or leucine residue (Fig. S3 *A* and *B*). These mutated *psbA3* genes were then transformed into the TD34 strain, resulting in the construction of three new strains in which only the modified *psbA3* is expressed. The resulting transgenic strains were then grown photoautotrophically in the presence of the remaining two antibiotics (Fig. 2*A*), and the mutations in each strain were verified by PCR, restriction enzyme cleavage (Fig. S3*B*) and DNA sequencing. As a control, the unmodified *psbA3* gene was introduced into the TD34, creating the RSS strain. In order to verify that the four protein complexes of the photosynthetic membrane accumulate in the mutagenized strains, immunoblot analysis of thylakoids proteins using specific antibodies for representative proteins in each complex was carried out. The results (Fig. 2*B*) show a similar accumulation of PSII (the D1 and D2 proteins), PSI (subunit I), cytochrome b_6f (Rieske protein), and ATP synthase (subunit β). The TD34 strain, in which

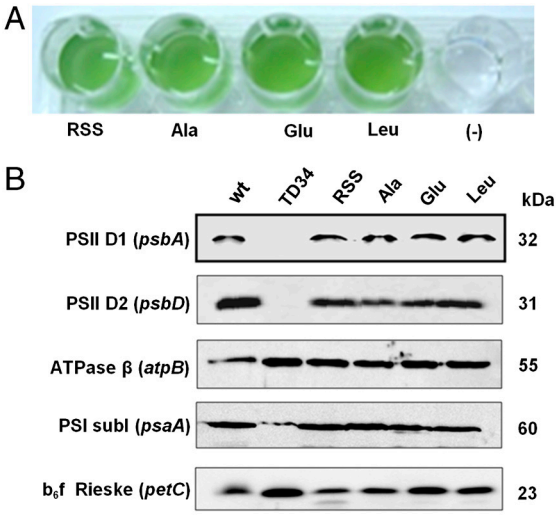

Fig. 2. Engineering of K238 mutant strains that grow photosynthetically. (*A*) Selection for photosynthetic growth of mutant strains. After transformation, cells were grown on BG11 media supplemented with antibiotics (kanamycin and chloramphenicol). Mutant strains are indicated below each well. (*B*) Immunoblot of isolated thylakoid membranes (1 μg chlorophyll/lane). Strains are indicated on the top of each lane. The antibodies probed for targets representing the major photosynthetic complexes in the thylakoid membrane (indicated on left). The TD34 strain, lacking all three *psbA* genes and therefore the PSII, is also deficient in the amount of PSI.

the three members of the *psbA* gene family were inactivated and thus no D1 protein is translated, lacks the entire PSII as represented here by the lack of the D2 protein. In addition, the amount of PSI is significantly reduced in this strain (Fig. 2*B*). All three viable mutants displayed whole cell oxygen evolution and isolated membrane 2,6-dichlorophenol indophenol (DCPIP) reduction rates that were 70–90% of the RSS strain (Fig. S4*A*). Thus, when normalized to chlorophyll content, maximal photosynthetic electron transfer rates were decreased in the mutants; however, this decrease had only a small effect on the rate of cell growth (Fig. S4*B*).

During normal PSII activity, D1 is damaged and replaced by an intricate protein synthesis system that prevents the loss of other PSII proteins (12, 32, 33). Damage to D1 has been suggested to be caused by radicals formed within the RC that result from the elevated redox potential required for electron abstraction from water (12). In order to see if the site directed lesions introduced into D1 affected the turnover process, *Syn* strains were labeled with a short pulse of ^{35}S-methionine followed by illumination in the presence of unlabeled methionine. The rate of D1 degradation and turnover was quantified by autoradiography and immunoblotting (Fig. S5*A–C*). The RSS, Ala, Glu, and Leu mutants displayed a similar rate of D1 degradation, implying that the degradation machinery is equally capable of processing damaged wt D1 and mutated proteins. That the degraded D1 is replaced by a new translated one is evident since the total amount of this protein, as determined by immunoblot analysis using specific antibodies, remained constant through the experiment (Fig. S5*B*).

Electron Transfer from H_2O to Cytochrome C Through Q_A Occurs in Glu but Not in the Other Mutant Strains. Having introduced a potential binding site into D1 without harming photosynthetic growth, a potential electron carrier was sought. Cyt c is an electron shuttle in many bacteria and mitochondria (25). We incubated oxidized horse-heart mitochondrial cyt c with thylakoid membranes isolated from the RSS and mutant strains under white light illumination (1,000 μE/(m^2 · sec)). Only when thylakoids of the Glu mutant were used could a significant increase in the cyt c α peak at 550 nm be observed, indicating light-dependent reduction of cyt c (Fig. 3). Addition of DCMU, which blocks electron transfer from Q_A to Q_B, increased the rate of cyt c reduction from approximately 12 to 20 μmole cyt c/(mg chl · hr) (Fig. 3, inset). Thylakoids isolated from the RSS strain displayed only limited ability to photoreduce cyt c (and only in the presence of DCMU), indicating that this phenomenon was acquired by the Glu mutation. The neutral mutation strains (Ala and Leu) showed cyt c reduction rates similar to the RSS strain. These results show that we have successfully engineered a cyt c binding site that is also a conduit for ET from Q_A to cyt c, which has a negligible effect on cell growth.

In order to verify that the observed cyt c photoreduction was directly related to electrons originated from H_2O, transferred through the PSII components, and abstracted from Q_A, we measured the light-dependent oxygen evolution of isolated thylakoids with either DCPIP or cyt c as electron acceptors in the absence or presence of DCMU, which prevents Q_B reduction (Fig. 4). When thylakoids isolated from either the RSS or the Glu strains were illuminated in the present of DCPIP, light-dependent O_2 evolution was completely inhibited by DCMU, indicating normal ET from water to Q_B. The O_2 evolution activity of the Glu thylakoids was about 70% of that obtained from RSS when normalized to the amount of chlorophyll. No O_2 evolution activity could be measured when RSS thylakoids were illuminated with cyt c serving as the electron acceptor. However, the light-dependent ET from water to cyt c of the Glu strain (in the presence of DCMU) exhibited comparable rates to those obtained with DCPIP. The maximal rate of cyt c reduction could be ascertained in this fashion. Because four cyt c molecules are reduced for

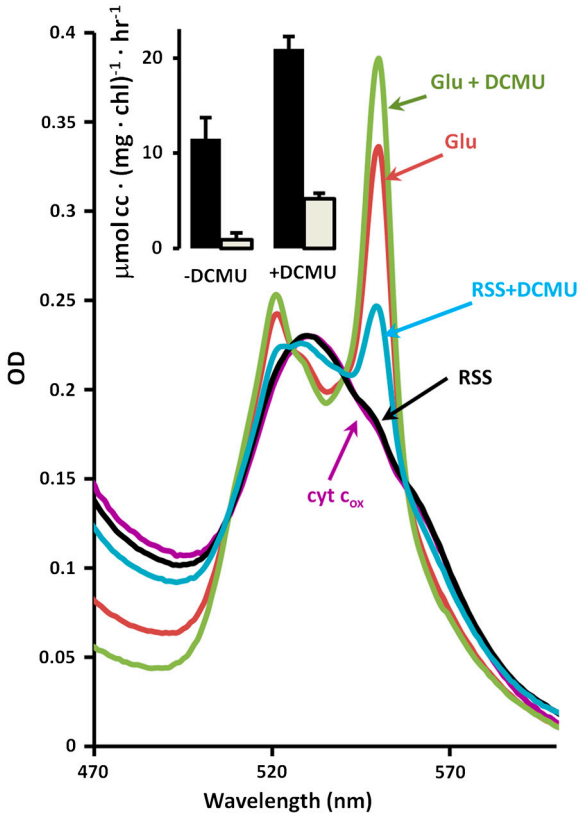

Fig. 3. Cytochrome c is photoreduced by Glu strain membranes. RSS or Glu thylakoid membranes in the presence or absence of DCMU were illuminated in the presence of oxidized cytochrome c for 4 minutes and the light–dark difference absorption spectrum was measured. cyt c_{ox}, spectra of oxidized cyt c, shown for reference. The inset panel shows a quantification of cyt c photoreduction by RSS (white bars) or Glu (black bars) membranes in three independent experiments in the absence or presence of DCMU.

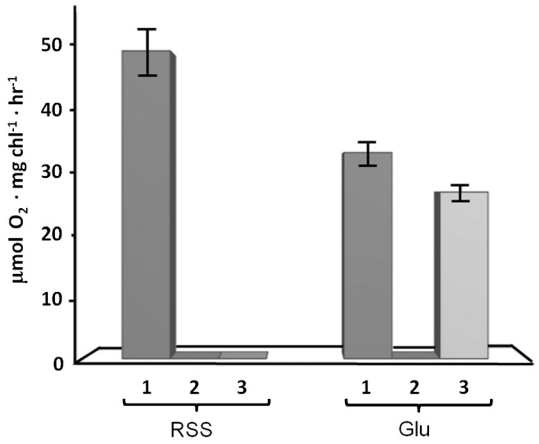

Fig. 4. Light-dependent electron transfer from H_2O to cyt c in the Glu strain. Oxygen evolution was measured by isolated thylakoids from the RSS and Glu strains. For samples 1 and 2, DCPIP served as the exogenous electron acceptor without (1) or with (2) the addition of DCMU. In sample 3, cytochrome c (in the presence of DCMU) was the exogenous acceptor.

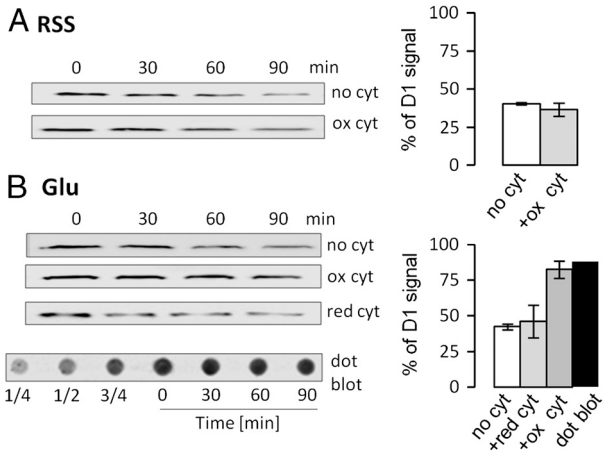

Fig. 5. The D1 is protected from photodamage induced crosslinking in illuminated thylakoids of the Glu strain supplemented with oxidized cyt c. Immunoblots of D1 in thylakoids isolated from the *Synechocystis* strains (RSS and Glu) illuminated for 0, 30, 60, or 90 minutes under light intensity of 850 µE/(m^2 s)), displaying the disappearance of D1 from the 32 kDa region of the SDS/PAGE. The membranes were illuminated either in the absence (no cyt) or the presence of oxidized (ox cyt) or reduced (red cyt) cytochrome c. In order to observe that the disappearance of the D1 from the 32 kDa region of the gel in illuminated thylakoids is not because of its degradation but rather by its crosslinking, thylakoids purified from the Glu mutant and illuminated as in panel B (no cyt) were analyzed by spotting on nitrocellulose membrane that was decorated with antibodies to the D1. In this method, the total amount of D1 in the membrane, including the noncrosslinked and the crosslinked photodamaged species, is determined. Quantification of the amount of D1 in the 32 kDa region of SDS/PAGE or the dot-blot following 90 min of illumination in three independent experiments is presented to the right.

every evolved oxygen molecule, the measured rate of 28 µmoles O_2/(mg chl · hr) is equivalent to 110 µmol cyt c reduced/(mg chl · hr), is similar to the rate of oxygen evolution from isolated thylakoid membranes in the presence of DCPIP as the electron acceptor (Fig. 4, compare Glu samples #1 and #3). Together, these measurements showed that in the Glu strain, the source of the electrons that reduce cyt c originate from water oxidized by PSII and transferred to Q_A. Because reduction of cyt c by electrons abstracted from water could not be obtained in the other strains, it can be concluded that this novel electron pathway is a result of the modification of the K238 residue to the negative charged glutamate. There is a difference between the cyt c reduction rate, measured by increase in the absorption of 550 nm (20 µmoles cyt c reduced/(mg chl · hr)) shown in Fig. 3 and by measuring the oxygen evolution rate (110 µmoles cyt c reduced/(mg chl · hr)) in Fig. 4. This difference indicates that during the measurement, the cyt c that was reduced is partially reoxidized, possibly by the presence of O_2 in the solution, or by a thylakoid bound factor (34).

Electron Transfer to Cyt C Protects D1 from Photo-Induced Cross Linking to Surrounding Proteins and PSII from Loss of Activity. The native process of ET in PSII is known to damage the reaction center, and we thus considered the possibility that the engineered ET conduit may function for only a short time due to the high degree of damage to PSII. When intact cells of cyanobacteria, algae, leaves, or intact chloroplast are illuminated, the D1 is rapidly degraded by the enzymatic degradation system. However, when purified thylakoids are illuminated, the enzymatic system that rapidly degrades the damaged D1 is inactive, or significantly inhibited, and as a result the damaged D1 is not removed by degradation but rather undergoes crosslinking to D2 and other PSII proteins (35). As aresult of this crosslinking, when assayed by immunoblot, the D1 disappears from the 32 kDa region of the gel and accumulates as a higher molecular weight crosslinked species. Prolonged illumination induces the formation of aggregates that are so large they do not penetrate into the gel (Fig. S6) (32, 33, 35–38). We assessed the degree of photodamage in the different strains by comparing the disappearance rate of D1 from the 32 kDa region of the SDS/PAGE by immunoblotting. When thylakoids obtained from the RSS or Glu strains were subjected to high light, it was found that the D1 band diminished at the same rate resulting in the disappearance of more than 60% of the protein from the 32 kDa region (Fig. 5). In order to validate that in these experimental conditions most of D1 is crosslinked to high molecular weight complexes (and not degraded), the amount of all forms of D1, either crosslinked, full length noncrosslinked, or in degradation products, was assessed by immune detection of the protein in thylakoids applied to nitrocellulose membrane using a dot-blot apparatus (Fig. 5*B*). The results clearly show that about 90% of the amount of D1 remains in the thylakoids. Indeed, and as described before (37), when the immunoblots of these experiments were overexposed, the crosslinking of D1 to high molecular weight aggregates is readily observed (Fig. S6).

We then proceeded to compare the photo-induced loss of PSII activity (oxygen evolution with DCPIP as the electron acceptor) that occurs in the illuminated thylakoids of the RSS and Glu strains, either with or without oxidized cyt c. We found that when incubated with oxidized cyt c, Glu thylakoids remain almost fully active for 90 min, while in the absence of cyt c, Glu thylakoids loose more than 70% of their activity within 30 min (Fig. 6).

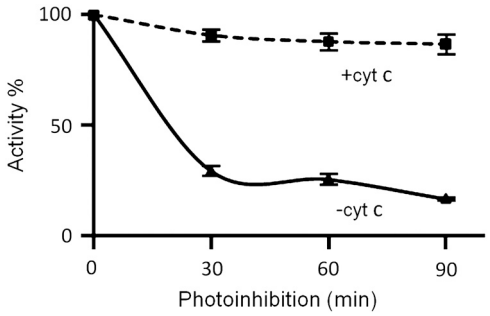

Fig. 6. Thylakoids of the Glu mutant are protected from photoinhibition when supplemented with cyt c. Thylakoid membranes of the Glu strain were illuminated at 850 µE/(m^2 · s) at 30 °C for the times indicated with the presence (dashed line) or absence (solid line) of cyt c. At each time point, an aliquot was removed and the rate of oxygen evolution was measured using DCPIP as the electron acceptor. 100% activity was as the same as shown for the Glu membranes in Fig. 4 sample #1.

RSS membranes lose a similar fraction of their activity in the absence or presence of cyt c. These results show that ET from Q_A^- to cyt c alleviates one of the major causes of photodamage to PSII.

Discussion

Critical Parameters Affecting the Photosynthetic Energy Conversion Machinery. All photosynthetic systems have three tuneable components that together provide an optimal yet flexible system for energy conversion: (*i*) Efficient light absorption, performed by pigments bound to the antenna light-harvesting complexes (LHC). (*ii*) Tuning of the LHC-RC cofactors to enable efficient transfer of the absorbed energy to enable charge separation. The potential for photochemistry by the RC chlorophyll molecules is a result of exquisite positioning of protein residues that tune the electronic state of the donor and nearby intermediate acceptor molecules. (*iii*) The internal electron transfer chain, on both the acceptor and donor sides of the primary donor, that must be insulated against spurious electron transfer to alternative acceptors. This is achieved by precise positioning of the correct chemical functionalities along the pathway and stabilization of reduced states. Insulation of the pathway is not a simple task, because certain amino acid side chains are quite amenable to electron transfer. All components of a photosystem must also posses the ability to self-assemble within its unique surroundings, which is achieved by protein-protein interactions and also by interactions between proteins and lipids in the membrane. The mixture of complementary protein surfaces (contributing rigidity to the cofactors) and the flexibility imparted by the lipid bilayer enable both exact positioning of the three previously described components and also afford the dynamic movements required to enable efficient forward electron transfer and inefficient back electron transfer. The additional requirement for proton translocation in PSII, whether it be through a series of residues (39) or via channels to the outer solvent (40), requires additional structural changes that must occur without disturbing the continued flow of electrons. The result of the optimization of aforementioned parameters make the possibility of changing or improving a photosystems activity in vivo or in vitro very difficult (41, 42). However, PSII is an attractive choice for possible manipulations because it simultaneously produces three important products: electrons, protons, and oxygen. When approaching the possible modifications of PSII one must also take into account its additional unique characteristics. The most important is the large redox potential required for water oxidation by the OEC. The resulting oxygen evolution could be the reason that PSII is highly sensitive to light, leading to the need for rapid turnover of the D1 protein, without which photosynthesis is rapidly lost. Utilizing a complicated system such as PSII outside of its native environment may result in some loss of functions due to unforeseen long-term effects. However, in the study presented here, we have successfully engineered a new electron transfer pathway and protein binding site into PSII (Figs. 1, 3, and 4) that does not lead to loss of cell viability (Fig. 2). By preserving photosynthesis, we envision that thylakoids with modified PSII can be used outside the living cell in potentially vast amounts and without the requirement of complicated isolation procedures.

The Positive Charge at Amino Acid Position 238 of D1 May Be Important for the Insulation of the PSII Electron Flow from External Oxidation by Soluble Species. The K238 position in the *Syn* PSII is conserved in all photosynthetic organisms and creates a positively charged patch in a general area of negative amino acids (Figs. 1 *B* and *C* and Fig. S1). The results of this work, revealing that replacing the positive charge with a negative amino acid enables the abstraction of electrons from Q_A, suggests that this positive charge may play an important role in the insulation of the electron flow chain from the oxidative reactions that could eliminate a fraction of electrons going to Q_B and therefore reduce the photosynthesis quantum yield. Such oxidants could be, for example, cytochromes or plastocyanin, both of which are generally positive, especially in the vicinity of their respective redox center. The positive charged amino acid could therefore provide the necessary insulation to prevent electron leaking to soluble oxidants. The conservation of the positively charged amino acid in higher plants (Fig. S2) suggests that this insulation may be required within plant or algal chloroplasts as well.

Photodamage to PSII Results with Crosslinking of the D1 Protein When Its Degradation Is Impaired. In illuminated intact cells or chloroplasts the D1 rapidly turns over (12), probably due to radicals produced by the photosynthetic electron flow. When PSII is exposed to conditions where the rapid turnover of the D1 is impaired, such as when isolated thylakoids are illuminated, the D1 is not degraded but rather cross linked and forms aggregates (32, 33, 35, 37). When the thylakoid proteins were analyzed by spotting the membranes on a nitrocellulose membrane and detection was performed using D1 specific antibodies, almost no reduction in its amount was observed (Fig. 5), indicating that the amount of D1 did not decrease, but rather it was crosslinked (Fig. 6). In this work, we used this phenomenon as an additional measure to analyze the degree of photodamage and the protection afforded by oxidized cyt c when incubated with the Glu strain. Our results show a clear correlation between the photoinhibition of electron flow (Fig. 6) and the degree of crosslinking of D1 (Fig. 5). Moreover, both parameters were significantly reduced when thylakoids from the Glu strains were illuminated in the presence of oxidized cyt c, indicating that the electron flow from H_2O to cyt c through Q_A, protected PSII from photodamage. Therefore, under such conditions thylakoids obtained from the Glu strain will preserve PSII activity for a much longer time than light-exposed wt thylakoids. This phenomenon may be important in a possible initiative aiming the using of thylakoids in a future designed energy producing biophotocell.

Materials and Methods

Strain and Culture Conditions. *Synechocystis* sp. PCC 6803 (wt), RSS and mutant strains were grown in BG-11 medium under white light (50 μE/(m^2 · sec)) at 27 °C. The triple mutant in which each one of the three *psbA* genes was replaced with a gene conferring resistance to antibiotics, TD34 (31) was grown in BG-11 medium supplemented with 5 mM glucose.

Cloning and Site Directed Mutagenesis. Genomic DNA was used to obtain a 1795 fragment containing the *psbA3* gene surrounded by 388 bp and 324 bp up and downstream respectively, termed the RSS fragment (Fig. S3*A*) by PCR using the oligonucleotieds shown in Table S1. This fragment was cloned and subjected to site directed mutagenesis using QuikChange (Stratagene) and the oligonucleotides displayed in Table S1. The wild type strain codon AAA coding for lysine was replaced by the codon GCA for Alanine, GAA for Glutamic acid or CTC for Leucine (Fig. S3*A*). The plasmids carrying the mutant *psbA* were transformed into the TD34 strain (31).

Thylakoid Membrane Isolation and Protein Blotting. The procedure for small scale thylakoid membranes preparation was described by Komenda et al. (43). The isolated thylakoids were analyzed by 12% SDS/PAGE containing 4 M urea. Proteins were then transferred to a nitrocellulose membrane, which was decorated with antisera against the PSII-D1, PSII-D2, the cytochrome b_6/f- Rieske Fe-S protein (Agrisera), the ATP synthase β subunit or the PSI-I protein (obtained from N. Nelson). For the analysis of the total amount of D1 in the membrane, including the crosslinked species, membranes (0.1 μg chl) were applied to nitrocellulose membrane using a dot-blot apparatus (44) and the amount of D1 detected by specific antibodies (Agrisera).

Photosynthetic Activity Measurements. ***DCPIP reduction rates.*** 5 μg chl of isolated thylakoids from wt or mutant strains were suspended in 50 mM MES PH = 6, 5 mM $MgCl_2$, and 15 mM NaCl and were incubated with 50 μM DCPIP at 30 °C for 30 sec in the dark. The absorption of the solution

was measured at 598 nm, prior to and following illumination with white light (1,000 $\mu E/(m^2 \cdot sec)$) for 50 sec.

Oxygen evolution rates. 1 ml of *Syn* cells of the different strains ($O.D_{730}$ = 1–2) were used for each measurement. The suspension was bubbled with N_2 and then incubated for 5 min at 28 °C in the dark. Rates of oxygen evolution were determined using a Clark-type electrode (Hansatech). Cells were illuminated with white light for 1 min followed by a 1 min dark interval, five times per sample, and the increase in oxygen concentration was measured digitally. The rate of oxygen evolution was calibrated accordiing to the manufacturers instructions with solutions bubbled with either N_2 (containing 0% O_2) or air.

Cytochrome c reduction. 5 μg chl of isolated thylakoids were incubated with 30 μM cyt c (Sigma-Aldrich) in buffer B and illuminated for 3–5 min with white light. The concentration of reduced cyt c was calculated using $\Delta\epsilon_{550-542} = 21\ mM^{-1}\ cm^{-1}$ obtained by a standard calibration curve.

Analyzing the rate of D1 photodamage induced crosslinking in illuminated thylakoids. Thylakoid membranes (30 μg chl/ml) were illuminated with light intensity of 850 $\mu E/(m^2 \cdot sec)$ at 30 °C in the absence or presence of cyt c (0.17 mM)(Sigma). The amount of the remained noncrosslinked D1 was analyzed by western blot and quantification of the signal in the 32 kDa region while the total amount of D1 in the membrane (noncrosslinked and crosslinked) was determined by spotting the membranes on nitrocellulose membrane and decorating with D1 specific antibodies (44).

Molecular modeling. Calculation of all electrostatic potential surfaces were performed using the APBS (Adaptive Poisson-Boltzmann Solver) software package (45). The coordinates of the 3BZ1-1 PSII and the 1HRC cyt c structures were modified using PDB2PQR (46) to include hydrogen and partial charges, followed by surface calculation and visualization using the APBS plugin in Pymol (47). All electrostatic potentials are presented at ±15 kT/e. Virtual mutagenesis of D1-238 was performed using Pymol, and the mutated side-chains were positioned in the same orientation as that of K238.

ACKNOWLEDGMENTS. We would like to thank Wim Vermaas for the TD34 strain and Itzhak Ohad for stimulating discussions and help in the performance of auxiliary measurements on the mutants. We thank Yoram Gershman for his help with obtaining and growing the TD34 strain. This work was funded by grants from the Israel Science Foundation BIKURA fund (1046/06), the Israel Ministry of Science, the Technion V.P.R. funds, the Israel-Mexico Energy Research Fund, and the Phyllis and Joseph Gurwin Fund.

1. Nelson N, Ben-Shem A (2004) The complex architecture of oxygenic photosynthesis. *Nat Rev Mol Cell Biol* 5:971–82.
2. Nugent JH (1996) Oxygenic photosynthesis. Electron transfer in photosystem I and photosystem II. *Eur J Biochem* 237:519–31.
3. Cordes M, Giese B (2009) Electron transfer in peptides and proteins. *Chem Soc Rev* 38:892–901.
4. Gray HB, Winkler JR (2003) Electron tunneling through proteins. *Q Rev Biophys* 36:341–72.
5. Kalman L, Williams JC, Allen JP (2008) Comparison of bacterial reaction centers and photosystem II. *Photosynth Res* 98:643–55.
6. Axelrod HL, Okamura MY (2005) The structure and function of the cytochrome c_2: Reaction center electron transfer complex from Rhodobacter sphaeroides. *Photosynth Res* 85:101–14.
7. Fromme P, Grotjohann I (2008) Structure of photosystems I and II. *Results Probl Cell Differ* 45:33–72.
8. Barber J (2009) Photosynthetic energy conversion: natural and artificial. *Chem Soc Rev* 38:185–96.
9. Renger G, Renger T (2008) photosystem II: The machinery of photosynthetic water splitting. *Photosynth Res* 98:53–80.
10. Fufezan C, et al. (2007) Influence of the redox potential of the primary quinone electron acceptor on photoinhibition in photosystem II. *J Biol Chem* 282:12492–502.
11. Krieger-Liszkay A, Rutherford AW (1998) Influence of herbicide binding on the redox potential of the quinone acceptor in photosystem II: relevance to photodamage and phytotoxicity. *Biochemistry* 37:17339–44.
12. Adir N, Zer H, Shochat S, Ohad I (2003) Photoinhibition—A historical perspective. *Photosynth Res* 76:343–370.
13. Lomoth R, et al. (2006) Mimicking the electron donor side of photosystem II in artificial photosynthesis. *Photosynth Res* 87:25–40.
14. Kruse O, Rupprecht J, Mussgnug JH, Dismukes GC, Hankamer B (2005) Photosynthesis: A blueprint for solar energy capture and biohydrogen production technologies. *Photochem Photobio S* 4:957–70.
15. Nelson N, Yocum CF (2006) Structure and function of photosystems I and II. *Annu Rev Plant Biol* 57:521–65.
16. Li Y, Horsman M, Wu N, Lan CQ, Dubois-Calero N (2008) Biofuels from microalgae. *Biotechnol Progr* 24:815–20.
17. Dismukes GC, Carrieri D, Bennette N, Ananyev GM, Posewitz MC (2008) Aquatic phototrophs: Efficient alternatives to land-based crops for biofuels. *Curr Opin Biotech* 19:235–40.
18. Gouveia L, Oliveira AC (2009) Microalgae as a raw material for biofuels production. *J Ind Microbiol Biot* 36:269–74.
19. Angermayr SA, Hellingwerf KJ, Lindblad P, de Mattos MJ (2009) Energy biotechnology with cyanobacteria. *Curr Opin Biotechnol* 20:257–63.
20. Carroll A, Somerville C (2009) Cellulosic biofuels. *Annu Rev Plant Biol* 60:165–82.
21. Manzanera M, Molina-Munoz ML, Gonzalez-Lopez J (2008) Biodiesel: An alternative fuel. *Recent Pat Biotechnol* 2:25–34.
22. Conlan B (2008) Designing photosystem II: Molecular engineering of photo-catalytic proteins. *Photosynth Res* 98:687–700.
23. Adir N, et al. (1996) Crystallization and characterization of the photosynthetic reaction center-cytochrome c_2 complex from *Rhodobacter sphaeroides. Biochemistry* 35:2535–2547.
24. Axelrod HL, et al. (2002) X-ray structure determination of the cytochrome c_2: Reaction center electron transfer complex from *Rhodobacter sphaeroides. J Mol Biol* 319:501–15.
25. Moser CC, Dutton PL (1988) Cytochrome c and c_2 binding dynamics and electron transfer with photosynthetic reaction center protein and other integral membrane redox proteins. *Biochemistry* 27:2450–61.
26. Loll B, Kern J, Saenger W, Zouni A, Biesiadka J (2005) Towards complete cofactor arrangement in the 30 Å resolution structure of photosystem II. *Nature* 438:1040–4.
27. Guskov A, et al. (2009) Cyanobacterial photosystem II at 29-Å resolution and the role of quinones, lipids, channels and chloride. *Nat Struct Mol Biol* 16:334–42.
28. Ferreira KN, Iverson TM, Maghlaoui K, Barber J, Iwata S (2004) Architecture of the photosynthetic oxygen-evolving center. *Science* 303:1831–8.
29. Moser CC, et al. (2003) Length, time, and energy scales of photosystems. *Adv Protein Chem* 63:71–109.
30. Mulo P, Sicora C, Aro EM (2009) Cyanobacterial *psbA* gene family: Optimization of oxygenic photosynthesis. *Cell Mol Life Sci* 66:3697–710.
31. Nixon PJ, Rogner M, Diner BA (1991) Expression of a higher plant *psbA* gene in *Synechocystis* 6803 yields a functional hybrid photosystem II reaction center complex. *Plant Cell* 3:383–95.
32. Mulo P, Sirpio S, Suorsa M, Aro EM (2008) Auxiliary proteins involved in the assembly and sustenance of photosystem II. *Photosynth Res* 98:489–501.
33. Murata N, Takahashi S, Nishiyama Y, Allakhverdiev SI (2007) Photoinhibition of photosystem II under environmental stress. *Biochim Biophys Acta* 1767:414–21.
34. Molitor V, Peschek GA (1986) Respiratory electron transport in plasma and thylakoid membrane preparations from the cyanobacterium *Anacystis nidulans. FEBS Lett* 195:145–150.
35. Ishikawa Y, et al. (1999) Turnover of the aggregates and cross-linked products of the D1 protein generated by acceptor-side photoinhibition of photosystem II. *Biochim Biophys Acta* 1413:147–58.
36. Schuster G, Even D, Kloppstech K, Ohad I (1988) Evidence for protection by heat-shock proteins against photoinhibition during heat-shock. *EMBO J* 7:1–6.
37. Lupinkova L, Komenda J (2004) Oxidative modifications of the photosystem II D1 protein by reactive oxygen species: From isolated protein to cyanobacterial cells. *Photochem Photobio S* 79:152–62.
38. Yamamoto Y, et al. (2008) Quality control of photosystem II: Impact of light and heat stresses. *Photosynth Res* 98:589–608.
39. Paddock ML, Feher G, Okamura MY (2003) Proton transfer pathways and mechanism in bacterial reaction centers. *FEBS Lett* 555:45–50.
40. Koepke J, et al. (2007) pH modulates the quinone position in the photosynthetic reaction center from Rhodobacter sphaeroides in the neutral and charge separated states. *J Mol Biol* 371:396–409.
41. Khan MS (2007) Engineering photorespiration in chloroplasts: a novel strategy for increasing biomass production. *Trends Biotechnol* 25:437–40.
42. Spreitzer RJ, Salvucci ME (2002) Rubisco: Structure, regulatory interactions, and possibilities for a better enzyme. *Annu Rev Plant Biol* 53:449–75.
43. Komenda J, et al. (2000) Degradation of the photosystem II D1 and D2 proteins in different strains of thecyanobacterium *Synechocytis* PCC 6803 varying with respect to the type and level of psbA transcript. *Plant Mol Biol* 42:635–45.
44. Schuster G, Timberg R, Ohad I (1988) Turnover of thylakoid photosystem II proteins during photoinhibition of *Chlamydomonas reinhardtii. Eur J Biochem* 177:403–10.
45. Baker NA, Sept D, Joseph S, Holst MJ, McCammon JA (2001) Electrostatics of nanosystems: Application to microtubules and the ribosome. *Proc Natl Acad Sci USA* 98:10037–10041.
46. Dolinsky TJ, et al. (2007) PDB2PQR: Expanding and upgrading automated preparation of biomolecular structures for molecular simulations. *Nucleic Acids Res* 35:W522–5.
47. DeLano WL (2002) The PyMOL Molecular Graphics System. http://www.pymol.org.